Final report for S. Ratynskaia's short term mission 18.09-1.10.2013 entitled "Study of high energy prompt electrons produced during nanosecond laser-target interaction "

S. Ratynskaia[a], G. Dilecce[b]
a Division of Space and Plasma Physics, Association EURATOM-VR, Royal Institute of Technology KTH, Sweden
b Istituto di Metodologie Inorganiche e dei Plasmi, CNR - Bari , Italy

The short term mission was dedicated to the experimental campaign on the interaction of metal and dielectrics targets with a Nd:YAG laser beam (λ= 1064 nm, power density 10101011 W/cm2) carried out in an environment with finite Nitrogen pressure. The observed N2 spectra are unambiguous evidence of the existence of a source, arriving at the observation volume primary to the plume, which excites and ionizes the background gas. Such a source can be either prompt electrons or VUV radiation. The analysis revealed that prompt electrons would need energies in excess of 1 keV which is incompatible with any acceleration mechanisms relevant for such laser intensities. On the other hand, VUV radiation is strong enough to explain the observed spectra.

The results have been presented at the 12th International Conference on Laser Ablation (COLA 2013), held in 6-11 October 2013 in Ischia, Italy as a poster contribution by S. Ratynskaia, G. Dilecce, P. Tolias entitled "Nitrogen optical emission during nanosecond laser ablation of metals: prompt electrons or photoionization". The manuscript based on the results of this short term mission at CNR Bari and reported below in detail, is in preparation for the submission to the COLA 2013 conference proceedings published in peer-reviewed journal "Applied Physics A".

I. INTRODUCTION

Ablation of solid targets by nanosecond pulsed lasers of intensities above the threshold $I_{th} = 10^8 - 10^9$ W/cm^2 results in rapidly expanding partially ionized vapor clouds [1, 2]. Such plasma plumes are characterized by electron temperatures ranging from a fraction of eV [2] up to 20 eV [3, 4] and typical ion energies of hundreds of eV [3, 5, 6]. These high ion energies have been attributed to acceleration by an electric field presumably created by the escape of hot fast electrons breaking-up quasineutrality [3, 4, 7, 8].

It is now necessary to define the term "prompt electrons" as used hereafter; as prompt we identify electrons continuously emanating from the laser-matter interaction zone faster than the plasma plume. Scenarios of formation of such electrons as well as the value of their energy vary drastically in the literature. The mechanisms proposed range from electrons escaping an initially single temperature plasma cloud due to their higher mobility [9], to inverse Bremsstrahlung [7, 8, 10] and three-body recombination [7], or the combination of multiphoton absorption effects with acceleration due to space-charge effects [11].

Lack of direct observation of this subpopulation is a plausible reason for such a diversity in the prompt electron formation scenarios. In fact, only few experimental evidence of prompt electrons have been reported thus far [4, 11–13]. The conclusion that these electrons emerge from the interaction zone before the plume is based on observations of a negative pre-peak in time-of-flight (TOF) signals [4, 11, 12]. However, as pointed out in ref. [14], electrostatic measurements can be misleading, pertaining to the fact that the probe current might be induced, rather than collected, due to rapid charge release [15]. Moreover, for similar laser characteristics, reported TOF measurements are contradicting and can differ by more than one order of magnitude [4, 12, 13]. Nevertheless, the most convincing evidence of prompt electrons with energies of ~ 100 eV, well above the plume temperature, are those of refs. [13, 16], where they were detected up to five meters away from the target in the presence of background plasma.

To elucidate the physics of formation of such an electron group, experimental evidence concerning their number, details of the energy distribution (EEDF) as well as their dependence on the target material, laser intensity and wave-length are necessary. With this motivation we have initiated our dedicated spectroscopic studies of the background Nitrogen gas emissions. The ionization of the background gas as a proof of the high energy prompt electrons was used in ref. [12], where Nitrogen emissions of the First Negative System (FNS) and of the Second Positive System (SPS) (to be defined below) were observed. However, the potential of such observation was not fully exploited in that work, since (i) SPS emission was misinterpreted as "normally forbidden", while it is actually produced by electron impact excitation whose cross-sections are known, (ii) no information on the EEDF was deduced.

Our results revealed that there are actually two possible ionization sources; the prompt electrons described above and extreme UV/soft-x ray emission from the plasma plume. We interpret the experimental evidence in the light of both hypotheses and conclude that the second scenario is taking the place.

II. EXPERIMENTAL SET-UP

The vacuum system consists of a stainless steel chamber with a vertical linear motion feed-through, mounted

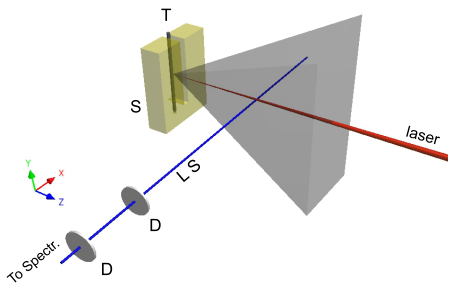

Figure 1: Scheme of the main experimental set-up. **T** target (2 mm diameter metal rod), **S** target screen, **D** diaphragm (1 mm diameter), **LS** line of sight (blue). The grey shadowed area is an indication of the propagation of the ionization source.

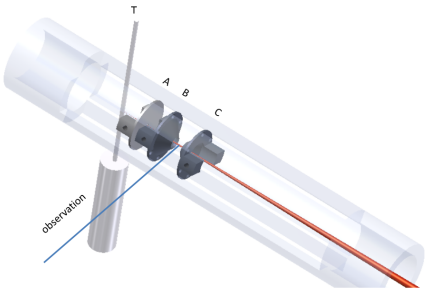

Figure 2: Scheme of the second experimental configuration. **T** target (2 mm dia. rod), **A** diaphragm (2 mm diameter), **B, C** diaphragm (6 mm diameter)

on the bottom side, on which the target is attached. The vacuum pump is a 150 l/s turbo dry pump. The base vacuum is 2×10^{-3} Torr. Nitrogen flux is controlled by a 100 sccm f.s. MKS mass flow controller. The minimum pressure achievable under 1 sccm flow is 5×10^{-3} Torr.

A schematic drawing of the experiment is reported in Fig.1. Most of the experiments reported here have been carried out with this configuration. The target is enclosed in a vertical screen, 4 mm wide, 8 mm deep, that limits the plume emission to an angle of 28° on the horizontal plane. The target with its screen is moved along the Y-axis by means of a motorized linear feed-through, with an up-down range of 2 cm. Another configuration has been built in order to apply an electrostatic field in a limited region in front of the target. Its schematic drawing is reported in Fig.2. Three diaphragms confine the laser-target plasma emissions into a cone defined by the first 2 mm diameter diaphragm located at 11 mm from the target. Between diaphragms A and B a potential difference of up to - 4 kV is applied. In order to avoid the ionization of the background gas, the voltage is pulsed by a fast HV switch, in such a way that it drops to zero just after the passage of the plume. Spectroscopic observations are localized between diaphragms B and C.

The linearly polarized laser beam is produced by a Nd:YAG laser at $\lambda = 1064$ nm, about 8 ns FWHM pulse duration. The beam energy used in the experiments is in the range of 10 - 325 mJ. The energy is varied by a half-waveplate and polarizer attenuator. The polarization is vertical, i.e. parallel to the wire target direction. The laser is focused on by a 50 cm focal length achromatic lens, but the target is set 3 cm away from the focal point, so that the beam diameter at the target surface is about 300 μm. The resulting fluence ranges from about 13 to 425 J cm^{-2}. Emission light is collected through a spatial filter composed of two aligned 1 mm diameter diaphragms, and then fed into an optic fibre which brings light into a monochromator (Spex 500M with 600 gr/mm grating, 300 nm blaze). The spatial filter can be moved along the Z-axis with a 8 cm range. The two outputs of the monochromator are equipped with an intensified CCD (ICCD) and a fast photomultiplier (PMT). The ICCD is gateable with minimum gate width of 5 ns, and is used for time-resolved spectra measurements. The gate delay generator of the ICCD is triggered by the laser Pockel's cell trigger. The PMT (Hamamatsu H10721-210) has a rise time of 500 ps. The PMT signal is measured by a 350 MHz bandwidth digital oscilloscope (1 ns rise time), whose acquisition is triggered by a fast (< 170 ps rise time) photodiode that captures a reflection of the laser beam.

III. RESULTS

A. Spectral analysis

Well before the plume arrival in the spectral observation region, strong emission from the nitrogen background gas are observed. These are the First Negative System (FNS) and the Second Positive System (SPS) emission. Possible mechanisms causing excitation and then emission are the electron impact, for both systems:

$$e + N_2(X^1\Sigma_g^+, v) \rightarrow 2e + N_2^+(B^2\Sigma_u^+, v') \rightarrow 2e + N_2^+(X^2\Sigma_g^+, v'') + h\nu_{(FNS)} \quad (1)$$

$$e + N_2(X^1\Sigma_g^+, v) \rightarrow e + N_2(C^3\Pi_u, v') \rightarrow e + N_2(B^3\Pi_g, v'') + h\nu_{(SPS)} \quad (2)$$

and photoionization for FNS only:

$$h\nu + N_2(X^1\Sigma_g^+, v) \rightarrow e + N_2^+(B^2\Sigma_u^+, v') \rightarrow e + N_2^+(X^2\Sigma_g^+, v'') + h\nu_{(FNS)} \quad (3)$$

with ionizing photon energy larger than 15.6 eV. The cross sections of electron impact processes (1- 2) are shown in Fig.3 [17]. Nitrogen photoionization cross sections in the photon energy range $\sim$ 20 - 50 eV are reported in [18], see Fig.4. Its value for $N_2^+(B^2\Sigma_u^+)$ direct excitation is around 1-2 Mb (10^{-18} cm^2).

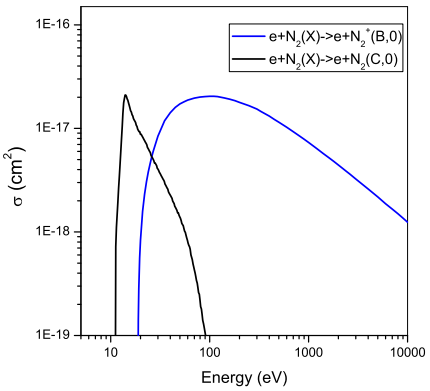

Figure 3: Cross sections for the electron impact processes that produce the measured nitrogen emissions.

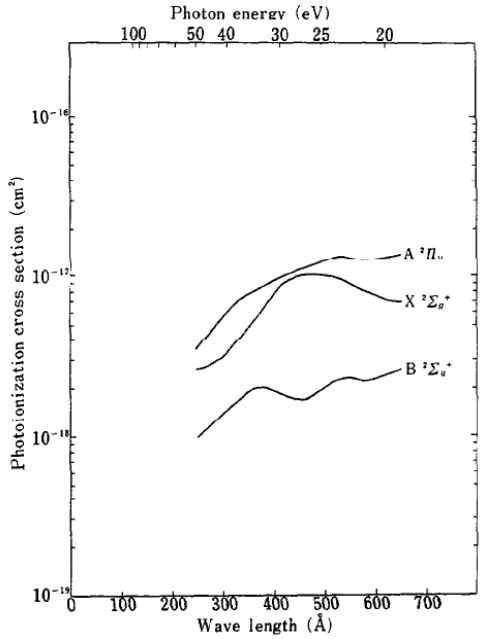

Figure 4: Partial photoionization cross sections for the production of N_2^+ in the states $X^2\Sigma_g^+$, $A^2\Pi_u$ and $B^2\Sigma_u^+$ [18].

A sample spectrum, with the SPS and FNS bands classification is shown in Fig.5. The time evolution of measured spectra is shown in Figs.6-7. The zero time is taken at the gate delay at which the emission starts to be observable.

Spectra are dominated by FNS emission. At the lowest possible pressure of 5 mTorr the strongest (0,0) SPS band starts to emerge from noise after 2 ns. The spectra time evolution shows an increase of SPS emission with time that is more pronounced with the increase of the background gas pressure, revealing the birth and growth with time/pressure of a group of electrons with energy below 100 eV that are able to excite the N_2(C) state. These

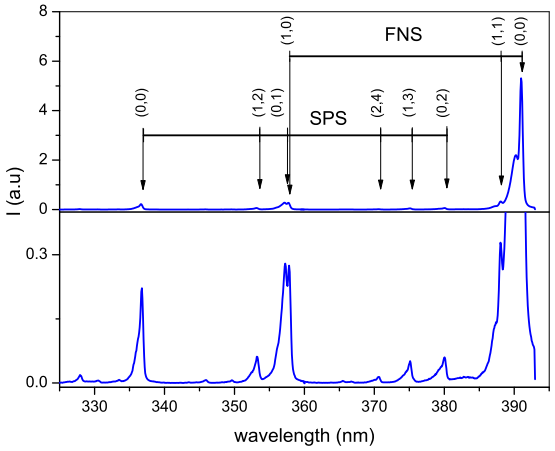

Figure 5: Emission spectrum in the 325 - 395 nm range taken at P = 20 mTorr, 16 ns after the laser pulse onset. In the bottom figure the vertical scale is changed in order to enhance the low intensity spectral features.

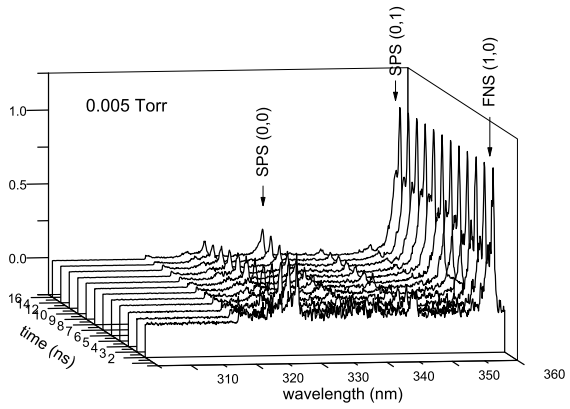

Figure 6: Spectra evolution at 5 mTorr, E_{las}=320 mJ. Spectra are normalized to the FNS(1,0) band intensity.

results are compatible with the picture of a primary excitation/ionization source that, as times goes, builds up a population of secondary low-energy electrons. If the primary source is a fast electron group, then the measured initial spectra and their time evolution are possible only if all nascent electrons are emanate with energies well above 100 eV.

B. Fluorescence pulses

The typical emission (fluorescence) pulse of the FNS (0,0) band spectral feature measured by the photomultiplier is shown in Fig.9. After the initial peak, followed by the radiative decay ($\tau \simeq 62ns$), the plume emission arrives. Fluorescence pulses (only their initial part) have

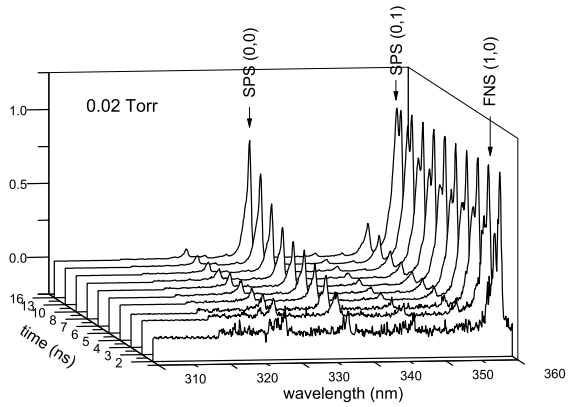

Figure 7: Spectra evolution at 20 mTorr, E_{las}=120 mJ. Spectra are normalized to the FNS(1,0) band intensity.

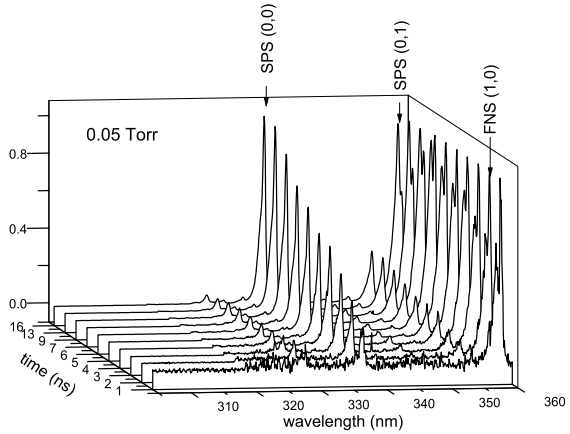

Figure 8: Spectra evolution at 50 mTorr, E_{las}=120 mJ. Spectra are normalized to the FNS(1,0) band intensity.

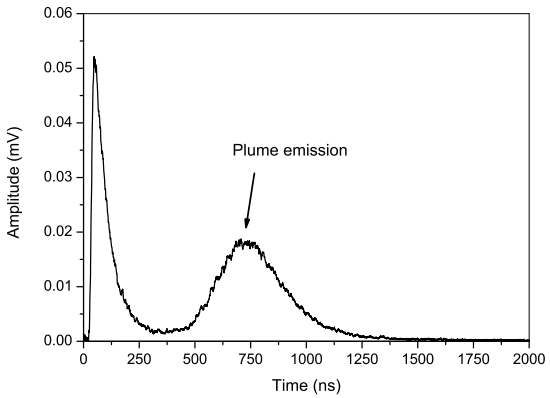

Figure 9: FNS (0,0) band fluorescence pulse, normalized to the maximum, at E_{las}=325 mJ and 5 mTorr pressure. The zero time position is arbitrary (see text).

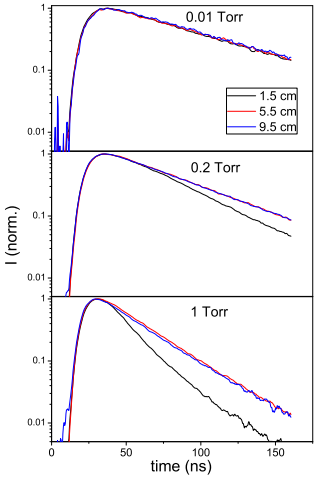

Figure 10: FNS (0,0) band fluorescence pulses, normalized to the maximum, at three distances from the target and three nitrogen pressure values. The zero time position is arbitrary (see text).

been measured at three distances from the target and three different pressures. Results are shown in Fig.10.

The fluorescence pulse is proportional to the time-dependent population of N_2^+(B,v=0). The latter (B) can be described by the equation:

$$\frac{dB}{dt} = RX - (Q(t)X + A)B\,, \qquad (4)$$

where X is the density of N_2(X) ground state, R is the excitation rate, A the radiative rate, and finally the collision quenching $Q(t) = Q_{N_2} + Q_{el}(t)$ is composed of a constant part due to collision with neutrals and a time-dependent part due to collision with low-energy electrons. The fluorescence rises until the excitation rate is larger than the loss rate. When the excitation falls below the loss rate and goes to zero, the fluorescence signal starts to decrease and then falls down with a rate equal to the quenching rate. Fig.10 reveals that the excitation lasts about 20 - 25 ns, i.e. at least as long as the laser pulse duration. The total loss rate is equal to the radiative rate at 0.01 Torr, while rising the pressure the collision quenching gives an increasing contribution. In particular, the time-dependent electron collision quenching is larger at higher pressure and closer to the target. The latter dependence is explained by the angular spread of the primary ionization source, that is limited to 28° in the X-Z plane and has no limitation in the Y-Z plane. Source is then much more intense close to the target, and more dense must then be the group of secondary low-energy electrons that contribute to $Q_{el}(t)$. This depends on time because of the recombination, that is faster at larger charge and neutral density. Further insight can be obtained by looking at the spatial/pressure dependence of the fluorescence intensity, reported in Fig.11.

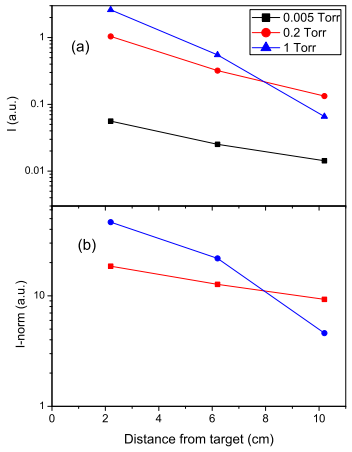

Figure 11: FNS (0,0) band intensity: (a) at three distances from the target and three nitrogen pressure values; (b) at 0.2 and 1 Torr, divided by the corresponding values at 0.01 mTorr.

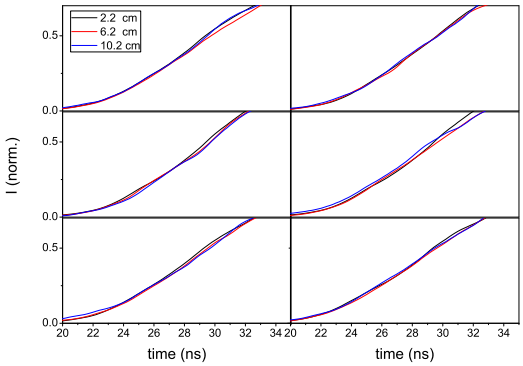

Figure 12: Rise of the fluorescence pulses at the three distances from the target at 5 mTorr. Six successive series of spatial scans are shown.

The intensity decreases moving away from the target and this decrease is more pronounced at higher pressure. Part of the decrease is due to the nascent angular spread in the Y-Z plane (light from the X-Z plane is totally captured by the spatial filter). At 5 mTorr the ionization mean free path of a 300 eV electron is about 30 cm. For higher energy it is slightly larger since the cross section decreases, see Fig.3. We therefore assume that the spatial dependence at 5 mTorr is representative of the nascent angular spread dependence, and report in Fig.11(b) the spatial dependence at 0.2 and 1 Torr divided by that at 5 mTorr, that should be representative of a pure pressure effect. We observe a decrease of a factor of 2 and 10 at 0.2 and 1 Torr.

C. Locality of spectroscopic measurements

The spatial filter has a great selectivity in the Y-Z plane and no selectivity along the X-axis. A doubt arises if part of the light collected at 6 and 10 cm might be due to reflections on the chamber walls of the much more intense emissions coming from the regions closer to the target. If this were the case it would be hard to explain why there is such a pronounced effect of the pressure on the spatial dependence of the intensity. In addition, the decay of the fluorescence pulse should not depend on the position, if the light source were the same for all positions. We conclude that the spatial selection is effective, and the locality of the measurements is reasonably assessed. Given the importance of this point, we nevertheless believe that it should be even more carefully addressed.

D. Time-Of-Flight analysis of fluorescence pulses

Time-of-Flight (TOF) measurements must be performed in a condition of low pressure in order to avoid any interference from secondary electrons and ensure that the excitation of FNS emission is caused by primary electrons only. The best condition available is at 5 mTorr. Fluorescence pulses at the three spatial positions are compared to assess if there is a clear delay in the onset of the pulse when moving away from the target. In Fig.12 six series of the spatial scans are shown. Repeated series show basically that the resolution of the measurement is below the necessary level, due to trigger instability, noise level, insufficient time response. If the prompt electrons are the primary source, a sub-ns delay over 8 cm would imply they have energy larger than 16 keV.

E. Fluence and target material dependence

The peak value of the first fluorescence pulse as a function of laser fluence is reported inFig.13, for six different metal targets. All targets show a similar dependence on fluence, with different absolute values.

F. measurements with a retarding electrostatic field

The results with application of a pulsed retarding electrostatic field between diaphragms A and B (see Fig.2) are very clear; no observable variation of the peak value of the FNS emission has been recorded up to the maximum available potential difference of -4 kV. Effects on nitrogen emission spectra are also insignificant: only a

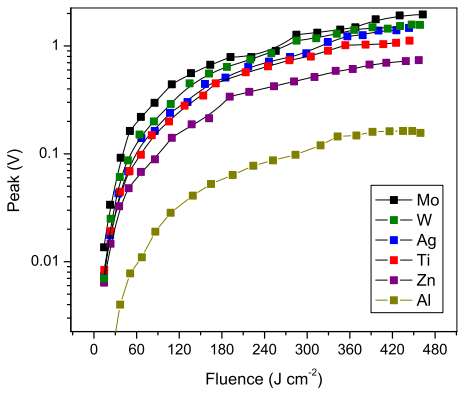

Figure 13: Peak value of the first fluorescence pulse as a function of laser fluence for various metal targets

slight decrease of SPS emission is observed in the condition of low pressure and initial times.

IV. DISCUSSION

A. Prompt electrons hypothesis

The hypothesis of prompt electrons emission as the primary source of excitation/ionization by electron impact processes must be compatible with the following observations:

- The nascent nitrogen spectra can be explain by a presence of a prompt electron group with energy in excess of some hundreds of eV, and no or absolutely negligible number of electrons at energies below 100 eV.
- TOF measurements can be explained only by a nascent energy (with directional motion) larger than 16 keV.
- The spatial dependence of the fluorescence intensity at larger pressures can be explained only by a loss of directionality of the primary electrons group by elastic collisions.
- The application of a retarding potential of 4 kV does not affect the FNS signal, indicating that the primary electrons must have an initial energy well above 4 keV. A possible effect on initial SPS emission might be ascribed to an influence of secondary electrons energy distribution.

The compatibility of the measured spectra time evolution with the prompt electrons hypothesis has been tested by means of a Monte Carlo simulation of an electron beam propagation into a gas medium. In particular, the model 'follows' the history of one electron in the energy space moving with a given initial energy and for a given time, and repeats the single electron calculation 10^6 times. This zero dimensional picture is equivalent to the passage of a primary electrons beam through a finite observation volume in the low pressure limit, i.e. provided the primary electrons do not loose a significant fraction of energy prior to reaching the observation volume. The model includes the ionization mechanism as well as the most important inelastic processes that contribute to electron energy losses. The number of electrons is not conserved, since ionizations produce secondary electrons whose kinetics is considered as well. An important aspect of the simulation is the energy distribution of electrons produced by ionization events. The distribution reported in [19, 20] have been used, in which most of secondary electrons are released at energies below 100 eV. The outcome of the model is an electron energy distribution function (EEDF) that evolves in time and from which the rate coefficients of processes 1 and 2 are calculated using the cross sections of Fig.3. The rate coefficients are then used as an input for Eq.(4), and in a similar one for $N_2(C)$ state, for the calculation of the time evolution of $N_2(B)$ and $N_2(C)$ states populations. These are finally used to simulate the spectra evolution using synthetic spectra generated by an appropriate software [21]. The simulated time evolution of nitrogen spectra shows a very good agreement with the measured one, with significant deviations only at 0.05 Torr, when the low pressure approximation is not more valid.

B. Photoionization hypothesis

Laser-target produced plasmas have been reported to produce extreme UV /softy X-ray radiation[22–24]. In Ref.[23], the absolute spectral intensities were measured. The results of such measurements for for a tungsten target are reported in Fig.14, for 800 mJ of laser energy focussed into a 50μm spot, corresponding to a fluence of about 4×10^4 Jcm^{-2} (i.e. about 100 higher than the maximum fluence in our experiments). The duration of UV emission has been reported in Ref.[22] to be the same as that of the laser pulse. We therefore conlcude that:

- The experimental time evolution of nitrogen spectra is compatible with the photoionization hypothesis. The radiation spectrum of Ref.14 shows abundance of above threshold radiation that leaves to the secondary electrons a kinetic energy of the order of some tens of eV. The physical situation can be described semi-quantitatively by the same Monte Carlo model as that used for prompt electrons, in which the primary source of excitation/ionization is photoionization with its rate coefficient.
- TOF measurements can be naturally explained by the propagation of the primary source at the speed of light
- The spatial dependence of the fluorescence intensity at larger pressures can be explained by photon

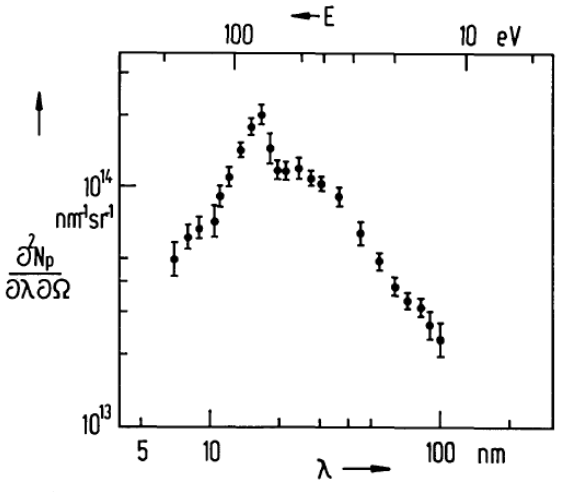

Figure 14: One pulse time integrated number of photons per unit wavelength and solid angle generated by a 800 mJ laser pulse irradiated onto a tungsten target with a 50μm spot [23]

absorption loss.

- The order of magnitude of the detected FNS peak signal agrees with calculations based on the spectrum of Fig.14. This calculation makes use of the absolute calibration of the optical detection system and of a scaling of the number of UV photons by the linear dependence of FNS emission peak value vs fluence measurements of Fig.13.
- The photoionization signal of the FNS emission is totally independent of any applied electrostatic field.
- A dependence on the target material has also been observed in Ref.[24].

V. CONCLUSIONS

The prompt electrons hypothesis as the primary source of excitation/ionization can be supported only if the initial energy of emitted electrons is directional and at least of the order of 10 kV. No acceleration mechanisms in this laser intensity regime can justify such hot electrons. Filamentation and parametric instabilities have higher intensity thresholds, while resonance absorption cannot lead to such energies. The photoionization hypothesis fits all the observations of this work, and appears to be the most reasonable explanation of the nitrogen background gas optical emissions.

We point out that the prompt electrons productions cannot be falsified by our measurements since their effect on nitrogen optical emissions production is negligible compared to that of photoionization. However, as pointed out in the Introduction, current literature reports electron energy of the order of some tens of eV, implying that such electrons should be able to produce SPS emissions. Estimations based on the spectra of Fig.6 and using the absolute optical collection system calibration, yield that the total number of prompt electrons - at energies larger than 11 eV - per pulse and pe solid angle cannot be larger than 10^6 srad^{-1}.

[1] S. Amoruso, R. Bruzzese, N. Spinelli, and R. Velotta. *J. Phys. B: At. Mol. Opt. Phys.*, 32:R131, 1999.

[2] B. Toftmann, J. Schou, T. N. Hansen, and L. G. Lunney. *Phys. Rev. Lett*, 84:3998, 2000.

[3] L. Torrisi, D. Mascali, R. Miracoli, S. Gammino, N. Gambino, L. Giuffrida, and D. Margarone. *J. Appl. Phys.*, 107:123303, 2010.

[4] S. Tudisco, D. Mascali, N. Gambino, A. Anzalone, S. Gammino, F. Musumeci, A. Scordino, and A. Spitaleri. *Nucl. Instrum. Meth. A*, 47:653, 2011.

[5] L. Torrisi, S. Gammino, L. Andò, and L. Làska. *J. Appl. Phys.*, 91:4685, 2002.

[6] Martinez R. Sierra B. Redondo C. Basterretxea F. J. Castano F. Ecija P., Sanchez Rayo M. N. *Phys. Rev. A*, 77:032904, 2008.

[7] N. M. Bulgakova, A. V. Bulgakov, and O. F. Bobrenok. *Phys. Rev. E*, 62:5624, 2000.

[8] F. Claeyssens, S. J. Henley, and M. N. R. Ashfold. *J. Appl. Phys.*, 94:2203, 2003.

[9] L. Torrisi and S. Gammino. *Rev. Sci. Instrum.*, 77:03B707, 2006.

[10] H. Cronberg, M. Reichling, E. Broberg, H. B. Nielsen, E. Matthias, and N. Tolk. *Appl. Phys. B*, 52:155, 1991.

[11] S. Amoruso, N. Armenante, R. Bruzzese, N. Spinelli, R. Velotta, and X. Wang. *Appl. Phys. Lett.*, 75:7, 1999.

[12] R. C. Issac, P. Gopinath, G. K. Varier, V. P. N. Nampoori, and C. P. G. Vallabhan. *Appl. Phys. Lett.*, 73:163, 1998.

[13] S. Vincena, W. Gekelman, M. A. VanZeeland, J. Maggs, and A. Collette. *Phys. Plasmas*, 15:072114, 2008.

[14] M. H. Hong and Y. F. Lu. *Appl. Phys. Lett.*, 76:248, 2000.

[15] M. H. Hong and Y. F. Lu. *Appl. Phys. A*, 69:S605, 1999.

[16] M. VanZeeland, W. Gekelman, S. Vincena, and G. Dimonte. *Phys. Rev. Lett.*, 87:105001, 2001.

[17] Y. Itikawa. *J. Phys. Chem. Ref. Data*, 35:31–53, 2006.

[18] Y. Itikawa, M. Hayashi, A. Ichimura, K. Onda, K. Sakimoto, K. Takayanagi, M. Nakamura, H. Nishimura, and T. Takayanagi. *J. Phys. Chem. Ref. Data*, 15:985–1010, 1986.

[19] C. B. Opal, W. K. Peterson, and E. C. Beaty. *J. Chem. Phys.*, 55:4100–4106, 1071.

[20] Y. Tzeng and E. E. Kunhardt. *Phys. Rev. A*, 34:2148–2157, Sep 1986.

[21] X Tan. Technical report, 2006.

[22] M. Kuhne. *Appl. Optics*, 21:2124–2128, 1982.

[23] J. Fischer, M. Kuhne, and B. Wende. *Appl. Optics*, 23:4252–4260, 1984.

[24] R. C. Spitzer, T. J. Orzechowski, D. W. Phillion, R. L. Kauffman, , and C. Cerjan. *J. Appl. Phys.*, 79:2251–2258, 1996.